Edgar A. Sanches^a, Sérgio M. de Souza^b, Ana Paola L. Carvalho^c, Graziella Trovati^d, Edson G. R. Fernandes^e, Yvonne P. Mascarenhas^e

Nanocomposite based on polyaniline emeraldinebase and α-Al₂O₃: A structural characterization

A ceramic-matrix nanocomposite based on polyaniline emeraldine base and aluminum oxide (PANI-EB/ α -Al₂O₃) was obtained by in-situ polymerization. X-ray diffraction pattern presented peaks related to both materials. The level of crystallinity was estimated at about 53 %. The average crystallite sizes of PANI-EB and α -Al₂O₃ were found to be \sim 40 Å and 570 Å, respectively. Scanning electron microscopy showed polymerization over ceramic particles. Fourier-transform infrared spectroscopy suggested physical deposition. The electrical conductivity of the PANI-EB/ α -Al₂O₃ nanocomposite was decreased by a factor of 80 when compared with that of pure PANI-EB. Therefore, the polymeric reinforcement and the ceramic matrix maintained their original structural features, but the electrical conductivity in the nanocomposite was reduced.

Keywords: Nanocomposite; Polyaniline; Aluminum oxide; α -Al₂O₃; Le Bail method

1. Introduction

Nanocomposites are expected to display unusual properties emerging from the combination of each component [1-4]. Different strategies have been employed along the years to prepare nanocomposites based on polymeric reinforcement. These materials can be classified in two different categories: physical encapsulation, in which the polymer is absorbed on the surface of inorganic particles, and chemical encapsulation, in which there is a covalent bonding between them [5-8].

Intrinsically conductive polymers (ICPs) have been extensively employed as reinforcement due to their great potential in technological applications [9–12]. Polyaniline (PANI) is one of the most studied ICPs due to low cost of the monomer, ease of synthesis/doping and chemical stability under ambient conditions. Polyaniline emeraldine-base (PANI-EB) is a successful example of polymer-doping that resulted in a conducting system in which the number of electrons remains unchanged (protonation) [13, 14]. Alumina (α -Al₂O₃), on the other hand, has a large surface area, adsorption capacity, good wear resistance, and is commonly used as a catalyst, filter, and filler for polymers to improve

mechanical barrier and conductive properties. Nanocomposites constituted of PANI and α -Al₂O₃ have been prepared employing different methods and many possible applications have been suggested [5, 15–18].

The great technological potential of polyaniline is masked by the disadvantages related to its insolubility and infusibility, as well as poor mechanical properties. To overcome this difficulty, procedures such as structural modification by ring or N-substitution, doping with functionalized protonic acids, blending with conventional polymers and nanocomposites, are considered as promising ways from an industrial point of view [7, 19–24].

In the present work, the nanocomposite PANI-EB/α-Al₂O₃, in powder form, was obtained by in-situ polymerization through polymeric oxidative chemical synthesis in the presence of α-Al₂O₃ particles. The crystal structure investigation of semi-crystalline materials is an important research topic in different areas. Many studies have been performed to characterize nanocomposites, but very few focus on structural characterization through structural refinement methods. Understanding the structure of semi-crystalline nanocomposites is essential for the development of new technological applications. The major contribution of this work is to obtain the cell parameters and crystallite size and shape using the Le Bail method applied to a semi-crystalline nanocomposite comprised of polymeric-reinforcement/ceramic-matrix. Fourier-transform infrared spectroscopy (FTIR) was used to obtain structural information related to the chemical bonds; X-ray diffraction (XRD) patterns were refined using the FullProf program package under the conditions of the method proposed by Le Bail; scanning electron microscopy (SEM) was carried out for the investigation of the nanocomposite morphology. Finally, these results were correlated with the obtained nanocomposite electrical properties.

2. Experimental

2.1. Nanocomposite synthesis

Dark blue nanocomposite made from polyaniline emeraldine-base and aluminum oxide (PANI-EB/ α -Al₂O₃) was synthesized based on previous works of Zhang [5] and Sanches et al. [17, 25] with some modifications. Aniline

^aLaboratório de Polímeros Nanoestruturados (NANOPOL), Federal University of Amazonas (UFAM), Manaus/AM, Brazil

^bLaboratório de Materiais (LABMAT), Federal University of Amazonas (UFAM), Manaus/AM, Brazil

^cDepartment of Materials Engineering, Federal University of Amazonas (UFAM), Manaus/AM, Brazil ^dInstitute of Chemistry of São Carlos (IQSC), University of São Paulo (USP), São Carlos/SP, Brazil

^e Institute of Physics of São Carlos (IFSC), University of São Paulo (USP), São Carlos/SP, Brazil

monomer was purchased from Aldrich and further distilled. $\alpha\text{-Al}_2O_3$ was obtained from Sapra/SA, São Carlos/SP, Brazil. Two different solutions were prepared. Solution I was prepared by dissolving 20 mL of distilled aniline in 300 mL of 1.0 M hydrochloric acid (HCl) and, subsequently, adding it to 167 g of $\alpha\text{-Al}_2O_3$ powder under stirring for 5 min. Solution II, on the other hand, was obtained by adding 11.5 g of ammonium persulfate (APS) to 200 mL of 1.0 M HCl. Solution II was added drop by drop to Solution I. The system remained under constant stirring for 3 h. Then, the dispersion was vacuum filtered and subjected to a solution of NaOH 1.0 M for 3 h to obtain the PANI-EB/ $\alpha\text{-Al}_2O_3$ nanocomposite powder.

2.2. FTIR

Infrared spectra were obtained at Nanomed Inovação em Nanotecnologia, São Carlos/SP, Brazil, in a Bomem-MB Series-Hartmann & Braun spectrophotometer in the range of 2000–500 cm⁻¹ and 16 scans. Samples were prepared in KBr pellets with mass ratio of 1:100.

2.3. XRD measurements and degree of crystallinity

XRD data were obtained at the laboratory of X-ray crystal-lography of IFSC/USP – São Carlos/SP, Brazil, using a Rigaku rotaflex diffractometer equipped with graphite monochromator and rotating anode tube, operating with Cu-K_a, 50 kV and 100 mA. Powder diffraction patterns were obtained in stepscanning mode, $2\theta = 5-60^{\circ}$, step of 0.02° and 3 s/step, where θ is the Bragg angle. Degree of crystallinity was estimated utilizing the whole diffractogram pattern using routine software, separating and then measuring the integrated intensities from the crystalline and non-crystalline phases. The integration was carried out over the whole range $2\theta = 5^{\circ}$ to 60° . The estimated crystallinity (EC), in terms of percentage, is given by,

$$EC = 100 A_{\rm c}/(A_{\rm a} + A_{\rm c}) \tag{1}$$

where A_c and A_a are, respectively, the crystalline and non-crystalline integrated intensities [26].

2.4. Le Bail method

The Le Bail whole powder pattern decomposition method was performed using the software package FullProf [27]. All parameters were refined by the least-squares method [28]. The pseudo-Voigt function modified by Thompson-Cox-Hastings was used as the peak profile function [29]. Instrumental resolution function parameters were obtained from a lanthanum hexaborate standard, LaB₆. Aniline tetramer single crystal parameters obtained by Evain et al. [30] were used as initial parameters (a = 5.7328 Å, b =8.8866 Å, c = 22.6889 Å, $\alpha = 82.7481^{\circ}$, $\beta = 84.5281^{\circ}$ and $\gamma = 88.4739^{\circ}$). Aluminum oxide structural parameters obtained by Lutterotti and Scardi [31] were used as initial parameters for alumina phase (a = 4.7605 Å, $\beta = 4.7605 \text{ Å}$, $\gamma = 12.9956 \text{ Å}, \ \alpha = 90.0^{\circ}, \ \beta = 90.0^{\circ}, \ \text{and} \ \gamma = 120.0^{\circ}).$ Spherical harmonics (SHP) [32] were used to account for the possible crystallite anisotropy; particle size was determined from the information on line profile (peak width and shape).

2.5. SEM analysis

SEM experiments were performed using a Supra 35, Carl Zeiss, at the Federal University of São Carlos (UFSCar), Brazil. Powder samples were deposited on a carbon tape and the surface morphology was analyzed at room temperature.

2.6. DC Electrical conductivity measurements

DC conductivity measurements were carried out at room temperature (300 K). The resistivities of PANI-EB and PANI-EB/α-Al2O3 were measured at the Institute of Physics at São Carlos (USP/IFSC), Brazil, using a Keithley Model 2612 A from 1 to 10 V. Powder samples were processed into pellets which were coated with silver ink. Electrical contacts were made in pellets using metal wires and silver paste.

3. Results and discussion

3.1. FTIR analysis

Absorption bands showed deformations and vibrations related to the interatomic bonds and, consequently, to the nanocomposite molecular structure. Figure 1 shows the FTIR spectra of PANI-EB, α -Al₂O₃, and nanocomposite.

The FTIR spectrum of PANI-EB showed main absorption bands at 1580 cm⁻¹, 1490 cm⁻¹, 1300 cm⁻¹, 1240 cm⁻¹, 1140 cm⁻¹, and 822 cm⁻¹. The peaks at 1580 cm⁻¹ and 1490 cm⁻¹ are assigned to the ring stretching vibration of quinoid and benzenoid, respectively [33, 34]. The peaks at 1300 cm⁻¹ and 1240 cm⁻¹ correspond to the N–H bending and C–C (or C–N) symmetric stretching modes, respectively. The bands at 1140 cm⁻¹ can be attributed to the inplane C–H bending modes. The C–H out-of-plane bending mode has been used as a key to identify the type of substituted benzene [35]. For PANI-EB, this mode is observed as a single band at 822 cm⁻¹, which falls in the range of 800–860 cm⁻¹ predicted for a 1,4-substituted benzene. Bands attributable to other types of substituted benzenes were not observed. Thus, the FTIR spectrum suggests the formation

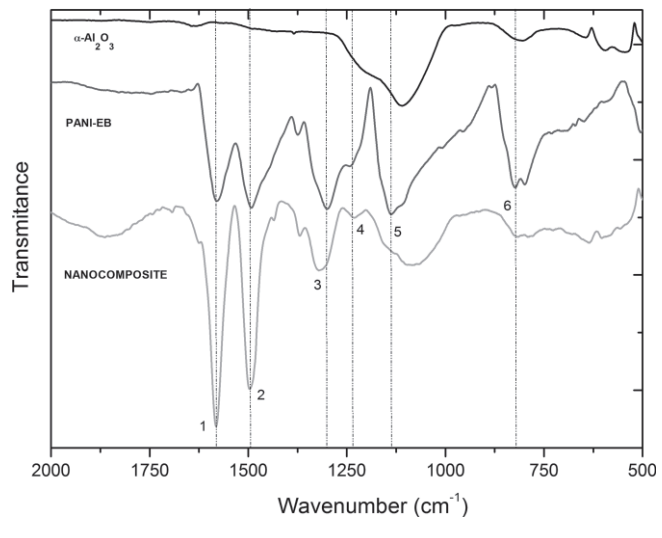


Fig. 1. FTIR of PANI-EB, α-Al₂O₃ and nanocomposite.

of PANI-EB with low degrees of branching and/or cross-linking. FTIR spectrum of α -Al₂O₃ is well known [36], showing bands between 649 cm⁻¹ and 457 cm⁻¹ corresponding to the AlO₆ octahedra condensates, which are the building blocks of α -Al₂O₃ structure.

The FTIR spectrum of the nanocomposite showed bands related to both materials. Additional bands indicating new chemical bonds to form the nanocomposite were not observed, suggesting physical deposition of PANI on the alumina plates. No chemical interaction was observed by Sanches et al. [17] either in a nanocomposite constituted of polyaniline emeraldine-salt form and α -Al₂O₃.

3.2. XRD measurements and degree of crystallinity

XRD was used for the fingerprint characterization of the semi-crystalline nanocomposite and the investigation of its structure in the crystalline phase. Figure 2 shows the semi-crystalline XRD pattern of PANI-EB and PANI-EB/ α -Al₂O₃.

The PANI-EB pattern presented more defined peaks up to $2\theta = 25^{\circ}$, showing a typical semi-crystalline XRD feature with broad peaks related to factors such as diffuse scattering due to the non-crystalline contribution, the nanoscale of the crystallites, and the superposed Bragg reflections. Peaks were observed at $2\theta = 6.8^{\circ}$, 10.1° , 15.4° , 20.8° , and 25.2° . The peaks located at larger angles are formed by many reflections (wider clusters). The peak located at $2\theta = 6.8^{\circ}$ is related to dependence of the molecular size of the counter ion [25].

The nanocomposite XRD pattern presented peaks of both phases. It is possible to discern narrow and intense peaks of α -Al₂O₃ from $2\theta = 25.7^{\circ}$, a typical characteristic of crystalline materials. This material yield a diffractogram with peaks at $2\theta = 25.7^{\circ}$; 35.2° ; 37.8° , 43.9° , and 52.6° .

The crystallinity in semi-crystalline materials is related to the aligned chains in the three-dimensional arrangement. Semi-crystalline nanocomposites based on polymer reinforcement/ceramic matrix are two-phase systems. The crystalline phase is attributed to the parallel and ordered polymer chains in a closely packed array (crystallites region) and to the highly ordered ceramic material. The non-crystalline

phase is attributed to disordered polymer chains without parallel alignment and to possible defects in the ceramic crystals. In polymeric materials, the crystalline domains, called crystallites, are much smaller than normal crystals and are interconnected with the non-crystalline regions. In contrast to the crystalline materials, which have well-defined patterns and larger crystallites, these polymers have broad overlapping Bragg reflection in a diffuse pattern. The occurrence of both kinds of characteristics is an evidence of the coexistence of ordered and disordered regions in the semi-crystalline nanocomposite.

The method developed by Hermans and Weidinger [37], and Goppel and Arlmann [38] was used for estimating the degree of crystallinity by means of X-ray diffraction pattern. The general procedure, shown in Eq. (2), is based on the law of conservation of intensity which states that the amount of intensity is determined by the integral over the volume for the square of the electron density:

$$\int I_{\rm s} dV_{\rm s} = \int \rho^2(r) dV_{\rm r} \tag{2}$$

The mean electron density is roughly the same for the non-crystalline and crystalline phases of a given semi-crystalline material, and it is possible to distinguish between them on the assumption that the intensity for the crystalline scattering is concentrated in the sharp reflections and that for the non-crystalline in the diffuse halo. The idea is to try to measure the integrated intensities from the crystalline and non-crystalline phases separately. The degree of crystallinity was estimated over the whole XRD pattern using Eq. (1) [26].

The nanocomposite crystallinity was estimated as $\sim 53\,\%$. Figure 3 shows the decomposition of the XRD pattern for crystallinity estimation. Sanches et al. [17] estimated the percentage of crystallinity to be around 70 % for a nanocomposite composed of polyaniline emeraldine-salt (PANI-ES) and $\alpha\text{-Al}_2O_3$. The crystallinity of pure PANI-EB is estimated to be ca. 30 % [39]. Thus, the crystallinity of the as-synthesized nanocomposite is larger than that of pure PANI-EB and smaller than that of pure $\alpha\text{-Al}_2O_3$, as expected.

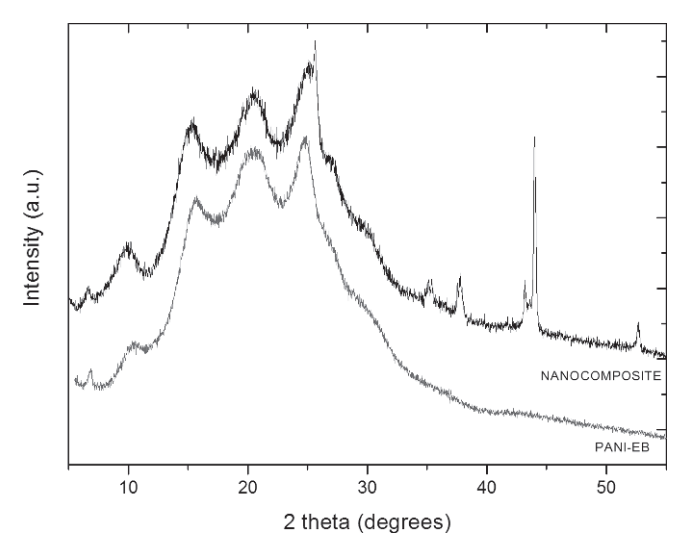


Fig. 2. PANI-EB and nanocomposite XRD pattern.

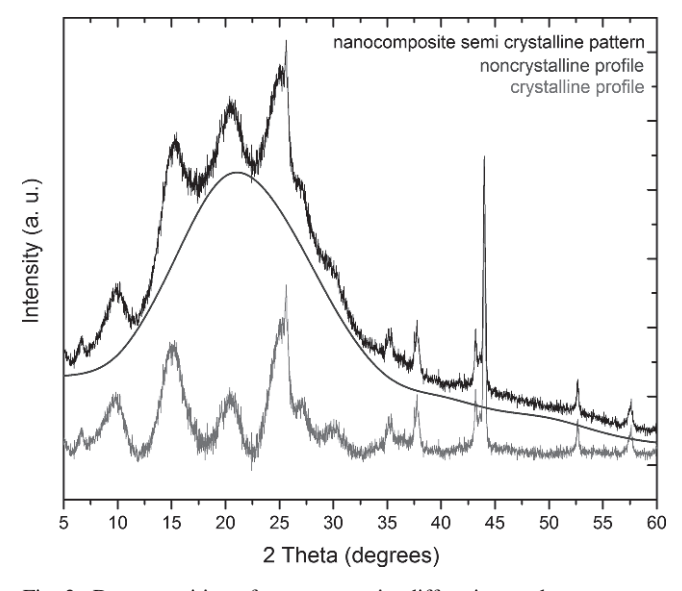


Fig. 3. Decomposition of nanocomposite diffraction peaks

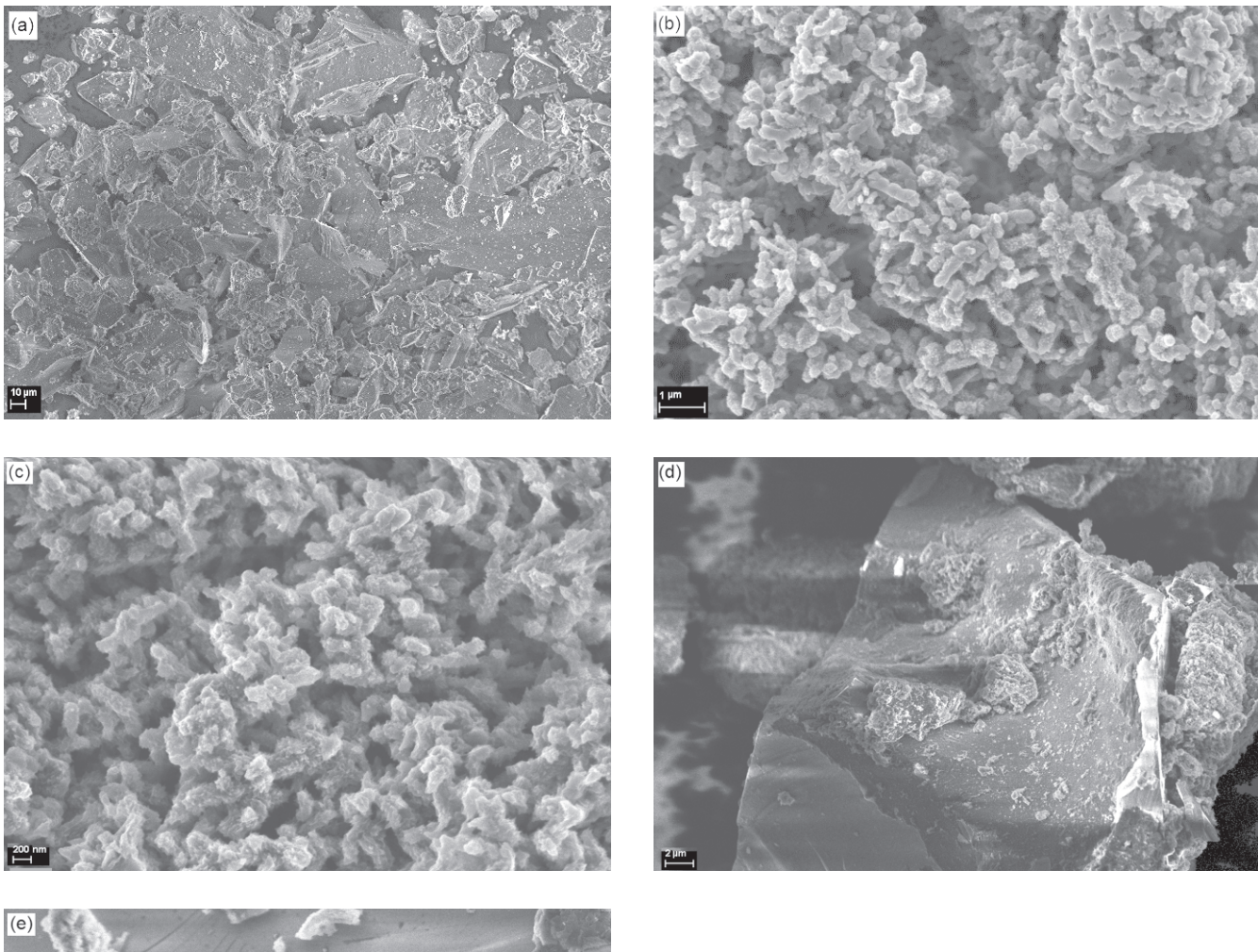
Int. J. Mater. Res. (formerly Z. Metallkd.) 106 (2015) 10

3.3. SEM analysis

From SEM, it was observed that the α -Al $_2O_3$ particles had a range of micrometric size with plate-like morphology (Fig. 4a). In PANI-EB images (Fig. 4b and c), nanosized particles with morphology similar to interconnected nanospheres were observed, which form the polymer nanofibers. In the nanocomposite PANI-EB/ α -Al $_2O_3$ images (Fig. 4d and e), it was observed that polymerization of PANI-EB occurred over alumina plates by physical deposition (as suggested by FTIR analysis), being possible to observe the morphology of both materials.

3.4. DC electrical conductivity measurements

The electrical conducting properties of nanocomposites are related to the properties of their components, the morphology of the system and the nature of the interface [40, 41]. In the case of conducting polymers such as polyaniline, the total conductivity is a function of inter-chain and intrachain mobility. The inter-chain mobility depends on the degree of crystallinity, temperature, and protonation (doping) level. In addition, the counter-ions are capable of introducing defects by causing significant charge polarization in neighboring chains [15].



(e)

Fig. 4. SEM images of (a) α -Al₂O₃; (b) PANI-EB; and (c) PANI-EB at higher magnification; (d and e) PANI-EB/ α -Al₂O₃ nanocomposite.

It is well known that polyaniline in the emeraldine ("half-oxidized") oxidation state can be reversibly switched between electrically insulating and conducting forms [42, 43]. However, even in the insulating form, the conductivity of PANI-EB can present considerably high values [39] and crystallinity can be as high as 50% [44]. On the other hand, alumina is an electrical insulator with DC electrical conductivity of about 10^{-14} S cm⁻¹.

The relationship between applied voltage and current is given by V = RI, where R, the factor of proportionality, is the nanocomposite electrical resistance. To verify the DC electrical conductivity (σ) of nanocomposite, the dimensions of pellet sample were considered, as given by the inverse of electrical resistivity (ρ) [45]:

$$\sigma = \frac{1}{\rho} = \frac{l}{RA} \tag{3}$$

where l is the pellet thickness, and A is the area of the straight section of the pellet. The slope of the I-V curve, shown in Fig. 5, provides the resistance (R) of the nanocomposite.

The DC electrical conductivity, σ , for pure PANI-EB shows different values in literature, depending on their methods of synthesis. Chaudhari and Kelkar [44] reported a conductivity of 5.27×10^{-7} S cm⁻¹ for undoped polyaniline by treatment of aqueous ammonia. Ozdemir et al. [46] found a value of 10^{-5} S cm⁻¹. Very recently, Sanches et al. [39] found a value of 1.32×10^{-7} S cm⁻¹ for PANI-EB obtained after neutralization of PANI-ES (previously obtained using HCl and ammonium persulfate) in NaOH 1.0 M.

In the present work, the DC electrical conductivity of $PANI-EB/\alpha$ - Al_2O_3 was obtained, by the average of three samples, to be around 1.57×10^{-9} S cm⁻¹. Thus we observe almost 80-fold decrease in the conductivity of the nanocomposite when compared with that of the pure sample of polyaniline in the emeraldine-base which is around 1.32×10^{-7} S cm⁻¹ [39]. Note that the matrix is composed only of insulating material and the PANI-EB contributes to an increase in nanocomposite electrical resistivity. The DC electrical conductivity for nanocomposite using polyaniline and a ceramic matrix also shows different values in literature depending on their methods of synthesis and the oxidation state of polyaniline. Nanocomposite formed by PANI-

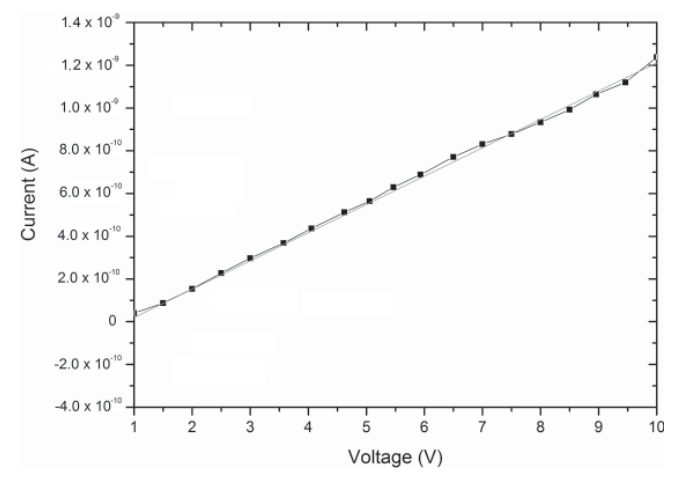


Fig. 5. Plot of *I* vs *V* for the electrical conductivity calculation.

ES and alumina showed DC electrical conductivity around 0.24 S cm⁻¹ (against 1.84×10^{-4} S cm⁻¹ for pure PANI-ES), presenting an increase of about 1300 times when compared with the pure PANI-ES at room temperature [17]. Su and Kuramoto [47] synthesized a processable PANI-EB/titanium dioxide nanocomposite with suitable conductivity (1–10 S cm⁻¹) that increased after thermal treatment at 80 °C for 1 h. However, Teoh et al. [18] obtained a decrease in DC electrical conductivity when they synthesized composite with nanofiber morphology by oxidative polymerization of aniline with alumina nanofibers.

Nanocomposites are closely related to the design of advanced devices for electronic and optoelectronic applications. The utility of polymer/inorganic particle nanocomposites in these areas is quite varied involving many potential applications that require conducting nanocomposites with electrical conductivity in the obtained range.

3.5. Le Bail method analysis

Following the Rietveld method [48] the *R* factors are related to the integrated intensities given by:

$$I_{k(\text{obs})} = \sum_{j} \left\{ w_{j \cdot k} \cdot S_{k(\text{calc})}^{2} \cdot y_{j(\text{obs})} / y_{i(\text{calc})} \right\}$$
 (4)

where $w_{j,k}$ is a measure of the contribution of the Bragg peak at position $2\theta_k$ to the diffraction profile y_i at position $2\theta_j$. The sum is overall $y_{j(\text{obs})}$, which can theoretically contribute to the integrated intensity $I_k(obs)$. So, there is a bias introduced here by the apportioning according to the calculated intensities; this is why the observed intensities are in fact said to be "observed" under quotes, in the Rietveld method. These "observed" intensities are used in the $R_{\rm B}$ and $R_{\rm F}$ calculations [49]. Basically the Le Bail method allows refinement of the unit cell parameters and microstructure parameters. In the traditional Rietveld method $S_k(calc)$ are the effectively measured intensities. In our case, however, they are only the intensities suggested by the profile fitting based on a distribution of intensities using a profile function [29] for each overlapped reflection constituting the few very broad peaks. These peaks are due to the low crystallinity and small crystallite size.

The Le Bail method [49–51] has recently been utilized to obtain structural information of semi-crystalline materials, even taking into account the large overlapped peaks on XRD patterns. Thus, it has been used to characterize some polymeric materials [52–55]. In order to perform the Le Bail method to investigate the crystal structure of the PANI-EB/ α -Al₂O₃ nanocomposite, the crystal symmetry and unit cell for PANI and aluminum oxide obtained, respectively, by Evain et al. [30] and Lutterotti and Scardi [31] were used as input data. Table 1 shows the refined parameters.

The refined lattice parameters were compared to those found in the literature [56, 57] which showed that both materials maintained their structural characteristics after forming the nanocomposite. It is known that the polyaniline synthesis conditions interfere in their physical and chemical characteristics. It was observed, in previous work [52], that the drop by drop reagent addition favored the appearance of the peak located at $2\theta = 6.8^{\circ}$, which typically corresponds to the large spacing induced when doped with a mo-

Refined Parameters	Evain et al. [30]	PANI-EB	Lutterotti and Scardi [31]	α -Al ₂ O ₃
a (Å)	5.7328(1)	5.7177 (2)	4.7605	4.7611 (2)
b (Å)	8.8866(2)	17.7678 (2)	4.7605	4.7611 (2)
c (Å)	22.6889(6)	22.7542 (2)	12.9956	12.9625 (2)
α (°)	82.7481(8)	82.9682 (2)	90	90
β (°)	84.5281(8)	84.5253 (2)	90	90
γ (°)	88.4739(11)	88.4306 (2)	120	120
$V(\mathring{A}^3)$	1 141.3(4)	2283.4 (4)	255.1	254.5
Global Average Size (anisotr.) (Å)	_	40 (4)	-	570 (50)
Crystallite Apparent size ₁₀₀ (Å)	_	47	-	560
Crystallite Apparent size ₀₁₀ (Å)	_	40	-	560
Crystallite Apparent size ₀₀₁ (Å)	_	34	-	270
$R_{ m wp}\left(\% ight)$	4.1			
$R_{\rm p}$ (%)	8.1			
χ^2	3.3			

Table 1. Comparison between the values found by Evain et al. [30] and Lutterotti and Scardi [31] with those found by PANI-EB and α -Al₂O₃, respectively.

lecule of larger molecular weight such as HCl. A better agreement was obtained by introducing a new "b" unit cell parameter valued around 17.77 Å [25, 56]. This peak is strongly dependent on the molecular size of the respective dopant used to induce crystallinity and electrical conductivity in polyaniline. During the neutralization process to obtain PANI-EB/ α -Al₂O₃, counter ions were not totally removed from the structure, and thereby the peak continued to exist.

Anisotropic size broadening can be written as a linear combination of spherical harmonics (SHP) and it is supposed that anisotropic size contributes only to the Lorentzian component of the total Voigt function. The explicit formula of the intrinsic integral breadth using the SPH treatment of size broadening is given by [57]:

$$\beta_h = \frac{\lambda}{D_h \cos \theta} = \frac{\lambda}{\cos \theta} \sum_{lmp} a_{lmp} y_{lmp} (\Theta_h \Phi_h)$$
 (5)

where β_h is the size contribution to the integral breadth of reflection (hkl), $y_{lmp}(\Theta_h\Phi_h)$ are real spherical harmonics with Θ_h and Φ_h being the polar angles of the vector h with respect to a Cartesian crystallographic frame [58] and a_{lmn} are refinable coefficients, depending on the Laue class. After refinement of the coefficients a_{lmp} , the program calculates the apparent size $(D_h, \text{ in Å})$ along each reciprocal lattice vector if the parameters $(U,V,W)_{instr}$ are fetched to the program from an external Instrumental Resolution Function file. It is important to stress that the standard deviation appearing in the global average apparent size is calculated using the reciprocal lattice directions, so it is a measure of the degree of anisotropy, and not of the estimated error. PANI-EB presented much smaller coherent scattering domains than alumina and the anisotropy model suggested a range of values. The average crystallite size obtained for PANI-EB is 40 Å with a standard deviation (anisotropy) of 4 Å. The apparent crystallite sizes in the directions [001], [010] and [100] were 34, 40 and 47 Å, respectively. The α -Al₂O₃ average crystallite size was found to be around 570 Å with a standard deviation (anisotropy) of 50 Å. There

is a largest apparent size of 560 Å in the [100] and [010] directions, and other smaller (270 Å) along [001].

4. Conclusions

We successfully synthesized a nanocomposite by in-situ polymerization based on polyaniline emeraldine base and α-Al₂O₃. Observations regarding the structural properties of the nanocomposite powder have been reported here. Rietveld refinement of XRD patterns was used under the conditions of the method proposed by Le Bail, enabling researchers to routinely use this tool in the study of semi-crystalline materials. The refined parameters are in agreement with those obtained in literature, except the "b" cell parameter, which was modified due to the dependence of the lattice parameters on the counter ion size. Particle size was determined from the information on line profile and showed that PANI-EB presented much smaller coherent scattering domains than alumina. XRD showed a semi-crystalline pattern with peaks related to both materials and degree of crystallinity of about 53 %. SEM analysis showed that PANI-EB was polymerized over the α -Al₂O₃ particles. FTIR showed an absence of chemical interaction between PANI-EB and alumina. Addition of α -Al₂O₃ particles during synthesis of polyaniline increased the nanocomposite resistivity.

The authors are grateful to the Brazilian Agency FAPEAM (Fundação de Amparo à Pesquisa do Estado do Amazonas) for the financial support to this work based on the Edital Papac 020/2013, and to the Prof. Dr. Puspitapallab Chaudhuri, from Federal University of Amazonas, for the critical reading of the manuscript.

References

- [1] P.M. Ajayan, L.S. Schadler, P.V. Braun: Nanocomposite Science and Technology, Wiley, New York (2003). DOI:10.1002/3527602127
- [2] P.H.C. Camargo, K.G. Satyanarayana, F. Wypych: Mater. Res. 12 (2009) 1. DOI:10.1590/S1516-14392009000100002
- [3] İ.Y. Jeon, J.B. Baek: Materials 3 (2010) 3654. DOI:10.3390/ma3063654

- [4] H. Karami, M.S. Mousavi, M.A. Shamsipur: J. Power Sources 117 (2003) 255. DOI:10.1016/S0378-7753(03)00168-X
- [5] D. Zhang: J. Appl. Polym. Sci. 101 (2006) 4372. DOI:10.1002/app.24326
- [6] A. Ahmed, A.D. Ahmed, S. Hashim, M.I. Khan: Pertanika J. Sci. Technol. 19 (2011) 329.
- [7] M.R. Nabid, M. Golbabaee, A.B. Moghaddam, A.R. Mahdavian, M.M. Amini: Polym. Compos. 30 (2009) 841. DOI:10.1002/pc.20628
- [8] S.X. Wang, L.X. Sun, Z.C. Tan, F. Xu, Y.S. Li: J. Therm. Anal. Calorim. 89 (2007) 609. DOI:10.1007/s10973-006-7569-3
- [9] S. Sathiyanarayanan, S.S. Azim, G. Venkatachari: Synth. Met. 157 (2007) 751. DOI:10.1016/j.synthmet.2007.08.004
- [10] S. Sathiyanarayanan, S.S. Azim, G. Venkatachari: Synth. Met. 157 (2007) 205. DOI:10.1016/j.synthmet.2007.01.012
- [11] G.M. Nascimento, V.R.L. Constantino, R. Landers, M.L.A. Temperini: Polymer 47 (2006) 6131. DOI:10.1016/j.polymer.2006.06.036
- [12] V. Petkov, V. Parvanov, P. Trikalitis, C. Malliakas, T. Vogt, M.G. Kanatzidis: J. Am. Chem. Soc. 127 (2005) 8805. DOI:10.1021/ja051315n
- [13] C.H. Chen: J. Appl. Polym. Sci. 89 (2003) 2142. DOI:10.1002/app.12361
- [14] E.T. Kang, K.G. Neoh, K.L. Tan: Prog. Polym. Sci. 23 (1998) 277. DOI:10.1016/S0079-6700(97)00030-0
- [15] N.P.S. Chauhan, R. Ameta, R. Ameta, S.C. Ameta: Indian J. Chem. Technol. 18 (2011) 118.
- [16] D.M. Sarno, S.K. Manohar, A.G. MacDiarmid: Synth. Met. 148 (2005) 237. DOI:10.1016/j.synthmet.2004.09.038
- [17] E.A. Sanches, A.S. Carolino, A.L. Santos, E.G.R. Fernandes, D.M. Trichês, Y.P. Mascarenhas: Adv. Mater. Sci. Eng. (2015) Article ID 375312. DOI:10.1155/2015/375312
- [18] G.L. Teoh, K.Y. Liew, W.A.K. Mahmood: Mater. Lett. 61 (2007) 4947. DOI:10.1016/j.matlet.2007.03.094
- [19] H. Namazi, R. Kabiri, A. Entezami: Eur. Polym. J. 38 (2002) 771. DOI:10.1016/S0014-3057(01)00232-4
- [20] P. Kar: Polyaminophenol: A substituted polyaniline derivative: Polyaminophenol: A substituted polyaniline with better processability and conductivity, Lambert Academic Publishing (2010).
- [21] N. Arsalani, M. Khavei, A.A. Entezami: Iranian Polym. J. 12 (2003) 237.
- [22] M. Lukasiewicz, P. Ptaszek, A. Ptaszek, S. Bednarz: Starch 66 (2014) 583. DOI:10.1002/star.201300147
- [23] M. Rashid, S. Sabir, A.A. Rahim, U. Waware: J. Appl. Chem. 2014 (2014), Article ID 973653. DOI:10.1155/2014/973653
- [24] J. Anand, S. Palaniappan, D.N. Sathyanarayana: Prog. Polym. Sci. 23 (1998) 993. DOI:10.1016/S0079-6700(97)00040-3
- [25] E.A. Sanches, J.C. Soares, A.C. Mafud, E.G.R. Fernandes, F.L. Leite, Y.P. Mascarenhas: J. Mol. Struct. 1036 (2013) 121. DOI:10.1016/j.molstruc.2012.09.084
- [26] P.G. Stern, E. Segerman: Polymer 9 (1968) 471. DOI:10.1016/0032-3861(68)90057-8
- [27] J. Rodríguez-Carvajal: Recent developments of the program Full-Prof, Commission on Powder Diffraction, IUCr, Newsl. 26 (2001).
- [28] G.S. Pawley: J. Appl. Crystallogr. 14 (1981) 357. DOI:10.1107/S0021889881009618
- [29] P. Thompson, D. Cox, J. Hastings: J. Appl. Crystallogr. 20 (1987) 79. DOI:10.1107/S0021889887087090
- [30] M. Evain, S. Quillard, B. Corraze, W. Wang, A.G. MacDiarmid: Acta Crystallogr., Sect. E: Struct. Rep. Online 58 (2002) o343. DOI:10.1107/S1600536802002532
- [31] L. Lutterotti, P. Scardi: J. Appl. Crystallogr. 23 (1990) 246. DOI:10.1107/S0021889890002382
- [32] N.C. Popa: J. Appl. Crystallogr. 31 (1998) 176. DOI:10.1107/S0021889897009795
- [33] S. Bhadra, N.K. Singha, D. Khastgir: J. Appl. Polym. Sci. 104 (2007) 1900. DOI:10.1002/app
- [34] C.A. Amarnath, S. Palaniappan: Polym. Adv. Technol. 16 (2005) 420. DOI:10.1002/pat.591
- [35] D.W. Hatchett, M. Josowicz, J.J. Janata: Phys. Chem. B 103 (1999) 10992. DOI:10.1021/jp991110z
- [36] A.E. Lavat, M.C. Grasselli: Adv. Technol. Mater. Mater. Process. J. 9 (2007) 103. DOI:10.2240/azojamo0242

- [37] P.H. Hermans, A. Weidinger: J. Appl. Phys. 19 (1948) 491. DOI:10.1063/1.1698162
- [38] J.M. Goppel, I.J. Arlmann: Appl. Sci. Res. A 1 (1949) 462. DOI:10.1007/BF02120311
- [39] E.A. Sanches, J.M.S. Silva, J.M.O. Ferreira, J.C. Soares, A.L. Santos, G. Trovati, E.G.R. Fernandes, Y.P. Mascarenhas: J. Mol. Struct. 1074 (2014) 732. DOI:10.1016/j.molstruc.2014.05.046
- [40] T. Ishikawa, M. Nakamura, K. Fujita, T. Tsutsui: Appl. Phys. Lett. 84 (2003) 2424. DOI:10.1063/1.1690493
- [41] G.A. Rimbu, C.L. Jackson, K. Scott, J. Optoelectro. Adv. Mater. 8 (2006) 611. DOI:10.1002/adem.200600048
- [42] A.A. Syed, M.K. Dinesan: Talanta 38 (1991) 815. DOI:10.1016/0039-9140(91)80261-W
- [43] A.G. MacDiarmid: Synth. Met. 84 (1997) 27.DOI:10.1016/S0379-6779(97)80658-3
- [44] H.K. Chaudhari, D.S. Kelkar. J. Appl. Polym. Sci. 62 (1996) 15– 18. DOI:10.1002/(SICI)1097-4628(19961003)62:1<15::AID-APP3>3.0.CO:2-V
- [45] S.A. Halperin: Evaluation Engineering 35 (1996) 49.
- [46] C. Ozdemir, H.K. Can, N. Colak, A. Guner: J. Appl. Polym. Sci. 99 (2006) 2182. DOI:10.1002/app.22718
- [47] S.J. Su, N. Kuramoto: Synth. Met. 114 (2000) 147. DOI:10.1016/S0379-6779(00)00238-1
- [48] H. Rietveld: J. Appl. Cryst. 2 (1969) 65. DOI:10.1107/S0021889869006558
- [49] A. Le Bail: Powder Diffr. 20 (2005) 316. DOI:10.1154/1.2135315
- [50] A. Le Bail, H. Duroy, J.L. Fourquet: Mater. Res. Bull. 23 (1988) 447. DOI:10.1016/0025-5408(88)90019-0
- [51] J. Rodríguez-Carvajal: IUCr Commission on Powder Diffraction, Newsl. 26 (2001) 12.
- [52] E.A. Sanches, J.C. Soares, A.C. Mafud, G. Trovati, E.G.R. Fernandes, Y.P. Mascarenhass: J. Mol. Struct. 1039 (2013) 167. DOI:10.1016/j.molstruc.2012.12.025
- [53] F.L. Leite, W.F. Alves, M. Mir, Y.P. Mascarenhas, P.S.P. Herrmann Jr., L.H.P. Mattoso, O.N. Oliveira Jr.: Appl. Phys. A: Mater. Sci. & Process. 93 (2008) 537. DOI:10.1007/s00339-008-4686-9
- [54] E.A. Sanches, L.C.A. Gomes, J.C. Soares, G.R. Silva, Y.P. Mascarenhas: Mol. Struct. 1063 (2014) 336. DOI:10.1016/j.molstruc.2014.01.082
- [55] A.S. Silva, J.C. Soares, A.C. Mafud, S.M. Souza, E.G.R. Fernandes, Y.P. Mascarenhas, E.A. Sanches: J. Mol. Struct. 1071 (2014) 1. DOI:10.1016/j.molstruc.2014.04.039
- [56] A.R. Hopkins, R.A. Lipeles, S.J. Hwang: Synth. Met. 158 (2008) 594. DOI:10.1016/j.synthmet.2008.04.018
- [57] J. Rodríguez-Carvajal, T. Roisnel: Mater. Sci. Forum. 123 (2004) 443
- [58] M. Casas-Cabanas, M.R. Palacín, J. Rodríguez-Carvajal: Powder Diffr. 20 (2005) 334. DOI:10.1154/1.2137340

(Received March 2, 2015; accepted June 5, 2015; online since August 3, 2015)

Correspondence address

Prof. Dr. Edgar Aparecido Sanches Universidade Federal do Amazonas (UFAM) Av. General Rodrigo Octávio Jordão Ramos 3000 – Campus Universitário – Setor Norte Coroado 69077000 – Manaus, AM Brazil

Tel.: +55 92 98416-7887 E-mail: sanches.ufam@gmail.com

Bibliography

DOI 10.3139/146.111280 Int. J. Mater. Res. (formerly Z. Metallkd.) 106 (2015) 10; page 1094–1100 © Carl Hanser Verlag GmbH & Co. KG ISSN 1862-5282